Geology of Lagoa das Furnas, a crater lake on São Miguel, Azores archipelago

Licentiate thesis

by

Tommy Andersson

Department of Geological Sciences

Stockholm University

2015

"Hot springs are prominent at Furnas and, along with its magnificent scenery…" (Moore, 1991)

Abstract

In this thesis, the results from a geophysical mapping and coring campaign of Lagoa das Furnas are presented. Specific focus is placed on the origin of a subaqueous volcanic cone mapped in the southern part of the lake. Lagoa das Furnas is a crater lake within the Furnas volcanic centre which is located on the island of São Miguel in the Azores archipelago. The Furnas volcanic centre has a long history of earthquakes and volcanic activity. The area is relatively well-studied, except for the lake floor. Therefore, a high resolution geophysical and geological mapping survey was conducted at Lagoa das Furnas. Sidescan sonar was used to map the surface of the lake floor and single beam sonar was used to acquire sub-bottom profiles. In addition to the geophysical mapping, sediment surface sampling and core drilling were carried out followed by geochemical analyses of the retrieved material. The mapped data permitted a characterisation of the floor of Lagoa das Furnas and revealed several volcanic features including fumarolic activity and a volcanic cone in the southern part of the lake. In order to unravel the origin of this cone several methods were applied, including analyses of tephra and minerals collected from the cone itself and from nearby deposits of two known eruptions, Furnas I and Furnas 1630. Sedimentological, petrological, geochemical and geochronological studies of pyroclastic deposits from the cone suggest a subaqueous eruption linked to the Furnas 1630 eruption. The chemistry of glass and crystal fragments sampled from the cone suggests that it is composed of more evolved magma than that of the main Furnas 1630, implying that the lake cone is likely a product of the last eruptional phase. According to historical records, two of three lakes were lost due the 1630 eruption. The results of this study show that the remaining lake is most likely Lagoa das Furnas and consequently did exist before the 1630 eruption.

Table of Contents

1 Introduction

1.1 Background

São Miguel is the most populated island in the Azores archipelago with ca. 150,000 inhabitants. Three active volcanoes on São Miguel have erupted within the past 500 years and the majority of the inhabitants live close to them. One of these, the Furnas volcano, is regarded as particularly dangerous with five explosive eruptions within 1,100 years (Moore, 1991b) Even a small eruption in the Furnas area could cause fatalities (Guest et al., 1999).

The Furnas area has been subjected to several geological studies. Booth et al. (1978) made a tephrochronology study and produced isopach and isopleth maps of tephra distributions during the past 3,000 years. Moore (1991b) made an overall geological study of Furnas. However, there are no systematic geological and geophysical studies of the crater lakes in São Miguel. Bottoms of crater lakes world-wide are generally less studied than their surrounding landscapes simply because the water body prevents direct mapping. Though, there is strong incentive to investigate and monitor crater lakes from a hazard mitigation perspective. Lakes situated in calderas are located above one or more magma chambers. Hot magma and storage of large volumes of water makes an explosive and dangerous combination. It can not only generate phreatomagmatic eruptions and lahars with devastating consequences, as during the large volcanic event that took place 1630 in Furnas (Cole et al., 1995), but also flooding when large amounts of water drain during an eruption. This may cause serious damage downslope from the crater lake, as when Aniakchak crater lake in Alaska rapidly drained because of caldera failure (Waythomas et al., 1996).

Geochemical investigations and monitoring of crater lakes are not too uncommon because they are considered a potential geohazards; e.g. seismic and fumarolic activity have been monitored at Poás Volcano in Costa Rica (Rowe Jr et al., 1992), gas discharges have been analysed at Mt. Ruapehu, New Zealand (Christenson, 2000) and temperatures and pH have been monitored in a newly formed crater lake at El Chichón in Chiapas (Casadevall et al., 1984). Some geochemical investigations of Lagoa das Furna's water have been carried out, as well. From these, Cruz et al. (2006) showed a high content of CO_2 in the water. Ferreira et al. (2005) monitored the fumarolic activity on the northern shore of Lagoa das Furnas and showed that CO_2 represented 94 to 99.6 mol % of the steam discharges.

Seismic and volcanic activities in crater lakes are widespread and common phenomena. The bottom of a crater may thus contain clues about a number of volcanic and tectonic processes affecting the area. These include caldera formation, collapse of the caldera-floor, dome- or cone-formation,

active faultings, fumarolic activity and active gas seepages. Lake bottom and/or sub-bottom structures may thus provide valuable information about the volcanic centre as a whole. Furnas valley has changed appearance during history. Historical documents reveal that more than one lake body existed in the Furnas area before the 1630 volcanic event, and studies of the lake bottom may reveal additional information about how the present Lagoa das Furnas got its form.

Sediment cores of deposits in a crater lake may provide an archive of past historical volcanic activity (Barker et al., 2000) and geophysical mapping using sonars may reveal geomorphological structures on the lake floor and within sub-bottom sediment stratigraphy (Ulusoy et al., 2008, Morgan et al., 2003). The aim of this licentiate project is to apply coring and geophysical mapping to characterize the bottom and sub-bottom of Lagoa das Furnas and to investigate the occurrence of tectonic events and volcanic activity that occurred since the Azores islands were first inhabited. In November 2012 a geophysical mapping survey was conducted and sediment cores were retrieved from the lake floor in June 2013 and May 2014. In this thesis the results from geophysical, sedimentological, petrological, geochemical and geochronological studies from the crater lake of Lagoa das Furnas are presented.

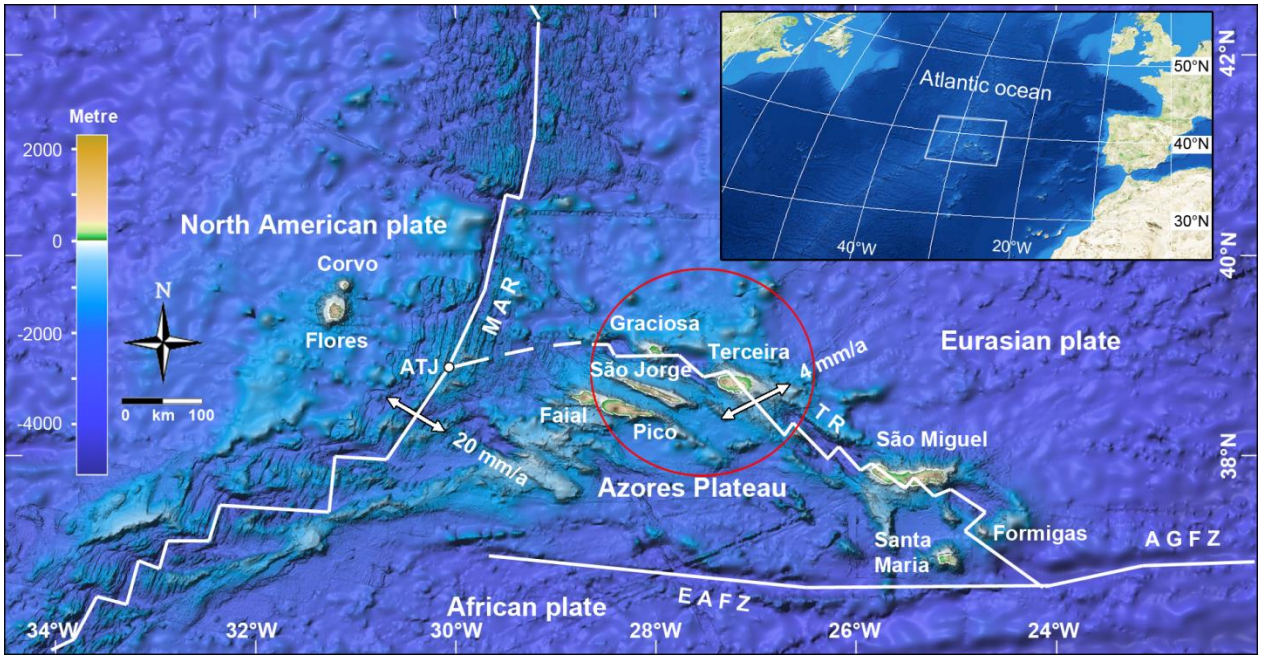

Fig. 1. *Bathymetric map of the Azores archipelago. The right inset shows the location of the archipelago in the North Atlantic Ocean. Major tectonic lineaments are shown with white lines and the dashed white line is an uncertain boundary (Yang et al., 2006), Mid Atlantic Ridge (MAR); Terceira Rift (TR); Azores Gibraltar Fracture Zone (AGFZ); East Azores Fracture Zone (EAFZ). The red circle shows the presumed location of a hot spot (Gente et al., 2003) and the small white circle shows the Azores Triple Junction (ATJ). Bathymetry is from EMOD net: http://www.emodnet-hydrography.eu/.*

1.2 Geological setting

1.2.1 Atlantic setting

Lagoa das Furnas is located on São Miguel, the largest island in the Azores archipelago (Fig. 1). The Azores archipelago comprises nine islands. The western group, Corvo and the smallest island Flores, is located on the North American plate, west of the Mid Atlantic Ridge (MAR) which has a spreading of ca. 20 mm/a (Vogt and Jung, 2004). Graciosa, Pico, Terceira, Faial and São Jorge belong to the central group. São Miguel and the oldest island Santa Maria form the eastern group together with the Formigas islets. Volcanism and earthquakes on the Azorean archipelago are directly related to their tectonic setting in the North Atlantic. The islands are situated on the Azores Plateau, which rises about 1,500 m above the surrounding seafloor. This plateau is formed at the Azores Triple Junction where the North American, Eurasian and African lithospheric plates meet with presumed hot spot interaction (Gente et al., 2003). At the plateau, the lithospheric plate boundary includes several additional complex tectonic features. One of the more significant is Terceira Rift, a hyper-slow spreading zone with plate separation of ca. 4 mm/a (Vogt and Jung, 2004). It starts from the Azores triple junction (ATJ) and extends along or alongside the islands Graciosa, Terceira and São Miguel. It is widely accepted, according to Vogt and Jung (2004), that the ATJ has made a jump from the intersection of East Azores Fracture Zone (EAFZ) and the MAR to its present location (Fig. 1).

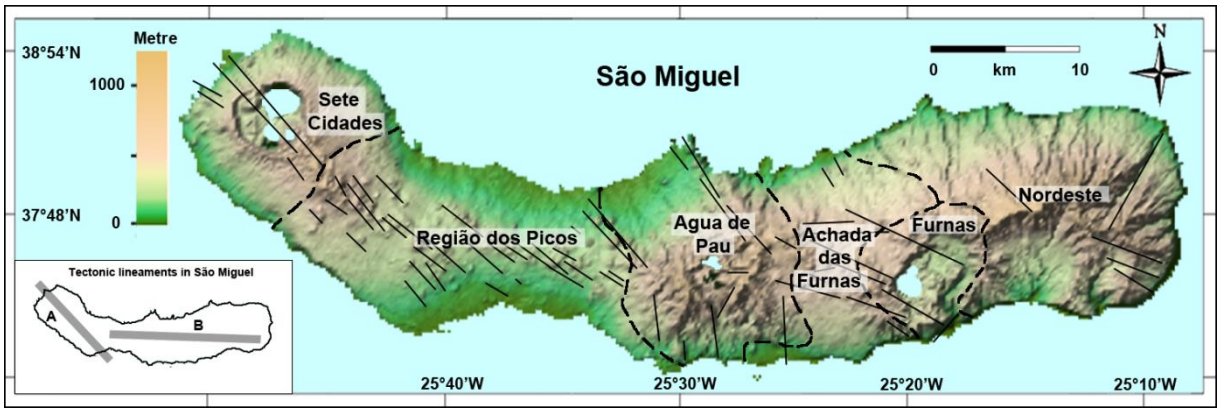

Fig. 2. *São Miguel island consists of six volcanic centres. Boundaries from Geological map of São Miguel (Moore, 1991a). Lines representing faults, inferred faults and volcanic alignments, modified from (Carmo et al., 2014).The inset shows the tectonic lineaments in São Miguel. A is the Terceira rift axis and B is the alignment of Agua da de Pau, Furnas and Nordeste volcanic centres, modified from (Beier et al., 2006). The topography is from the global land elevation model (DEM) generated from the Shuttle Radar Topography Mission (SRTM) (Farr et al., 2007).*

1.2.2 São Miguel setting

The Terceira rift axis crosses the western part of São Miguel where it trends NW-SW (Fig. 2), whereas in the central and eastern parts of the island, the rift trends W-E,

parallel to EAFZ (Beier et al., 2006, Moore, 1991a). This is expressed as a series of trachytic volcanic centres linked by rift zones. The island comprises a total of six

site of at least five eruptions, mostly within the caldera, during the past 5,000 years (Booth et al., 1978). A major eruption occurred ca. 5,000 years ago and is a key

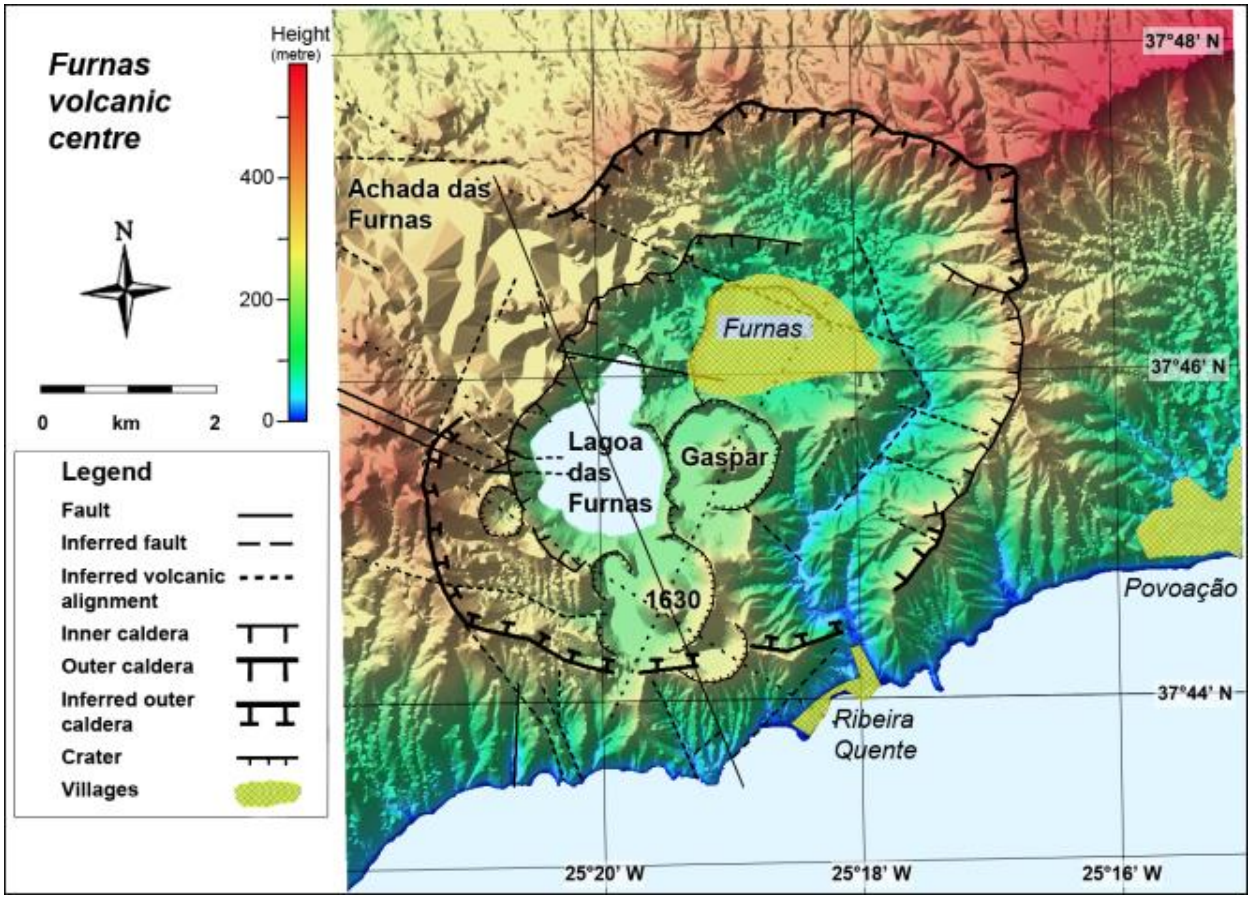

Fig. 3. *Map of the Furnas crater complex with the major tectonic and volcanic features marked. The locations of the dome of Pico do Gaspar and the dome from the 1630 eruption are shown. The fissure zones from Achada das Furnas front Lagoa das Furnas and permeate the caldera (Carmo et al., 2014). The most densely populated parts of Furnas area are check marked in yellow.*

volcanic zones. Sete Cidades is the westernmost of these zones. It is an active trachytic stratovolcano which has had at least 17 explosive eruptions during the past 5,000 years (Guest et al., 1999) (Fig. 2). Further east, Região dos Picos which is sometimes referred to as the "waist region" is an 18 km long rift field with numerous mainly alkali-basaltic cinder cones. These link to the next volcanic centre, Agua de Pau which is also called Fogo. This has been the

marker horizon in the area, called "Fogo A" (Walker and Croasdale, 1971). East of Fogo is Achada das Furnas, a fissure zone, dominated by alkali-basalt cinder cones and links with the active Furnas volcanic centre. The easternmost volcanic centre, Nordeste, is no longer active. Nordeste is between 4 to 0.95 million years old and is the oldest volcano centre in São Miguel (Abdel-Monem et al., 1975).

1.2.3 Furnas setting

The Furnas trachytic volcano centre is located approximately 800 m above sea level and is about 100,000 years old, making it the youngest of the active volcanos on the island (Moore, 1991b). The centre is transected by several WNW-ESE trending faults which extend from the Achada das Furnas rift zone (Guest et al., 1999) (Fig. 3). It consists of two craters with edifices that are not well developed; the outer caldera is about 30,000 and the inner caldera is about 10-12,000 years old (Guest et al., 1999). The formation of the inner caldera was probably followed by an eruption related collapse that could have formed the crater lake Lagoa das Furnas (Guest et al., 1999). During the past 5,000 years at least 10 intra caldera eruptions have occurred of trachytic character and formed pumice rings and domes on the caldera floor (Booth et al., 1978). Mafic eruptions have only occurred on the flanks of the caldera. Furthermore, three areas of fumarolic activity are found in the caldera. One is found on the northern shore of Lagoa das Furnas and probably related to the nearby fault. The other two areas are found in Furnas village and 1 km southeast of Ribeira Quente (Moore, 1991b).

1.3 Hazards in Furnas

At times, volcanism has plagued the islands situated along Terceira Rift zone (Malheiro, 2006, Lourenço et al., 1998, Searle, 1980). For example, the Furnas volcano has had eight trachytic eruptions, between 2,900 years BP and 320 years B.P. This gives a mean dormant time of ca. 370 years which means the next eruption may be overdue. Moreover, the mean dormant time for the last five eruptions, between 1,100 years BP and 320 years BP, is approximately 175 years which means that an eruption is now long overdue (Moore, 1991b). Mathematical calculation by Jones et al. (1999), based on Poisson distribution of the eruptions for the last 5,000 years, show that the risk of an eruption before 2099 is 53 % with a 95 % confidence interval.

Besides volcanism, the Furnas area is particularly vulnerable to geohazards related to landslides and degassing (Guest et al., 1999). The steep walls of the caldera enclose both the lake and the villages of Furnas and Ribeira Quente which limits evacuation routes for people in the case of volcanic eruptions, flooding or mass wasting (Fig. 5). The Furnas area has therefore been closely monitored with respect to geohazards over recent decades (Baxter et al., 1999, Gaspar et al., 2004, Ferreira et al., 2005).

1.3.1 Earthquakes

The Azores archipelago is an area of high seismic activity (Senos et al., 1998). One major earthquake occurred in 1757 and killed more than 20 percent of the population on São Jorge Island. The largest event during the 20th century occurred at Terceria Island 1980; the magnitude was 7.2 and caused many fatalities. An earthquake in 1998 had a magnitude 5.8 and caused severe damage in Faial and Pico (Senos et al., 1998).

São Miguel has high seismic activity (Guest et al., 1999). The area between Fogo and Furnas is the most seismically active on São Miguel (Gomes et al., 2006) (Fig. 4). Several catastrophic earthquakes have occurred in the Furnas area during the last five centuries. One of the most devastating occurred in 1522 and destroyed the former capital Vila Franca do Campo, ca. 10 km west of Furnas. Furthermore, more than 46,000 earthquakes were registered in the Congro-Fogo seismogenic region, ca. 7 km west of Furnas, between May and December 2005, the strongest had a magnitude of 4.3. Even though the earthquakes were of smaller size they trigged more than 250 landslides (Marques et al., 2007).

1.3.2 Landslides

The Azores are located in a mild maritime climate zone. The average temperature is 17.8°C and the annual average rainfall in the Furnas area is 2220 mm (Cruz et al., 1999). The soil in São Miguel is unconsolidated and contains tephra and pyroclastic rocks (Moore, 1991b). During long periods of rainfall, the soil can become saturated and landslides can occur either spontaneously or to be trigged by earthquakes (Valadão et al., 1999).

Several major landslides have occurred in São Miguel. For example the devastation of the former capital Vila Franca do Campo (1.3.3) was caused by an earthquake triggered landslide. This landslide killed the entire population of nearly 5,000 people. São Miguel was also plagued with heavy rain storms in October 1997, which most likely contributed to the landslides that killed 29 people in Ribeira Quente, situated in the south flank of Furnas (Figs. 3 and 5). Houses and bridges were destroyed and the area was isolated for more than 12 hours (Valadão et al., 1999).

The risk of landslides has been mapped for São Miguel Island showing that the highest risks occur along the southern shore of Furnas facing the ocean, although practically all slopes in the Furnas area are identified as high-risk areas (Valadão et al., 1999). Strong seismic activity is expected prior to a

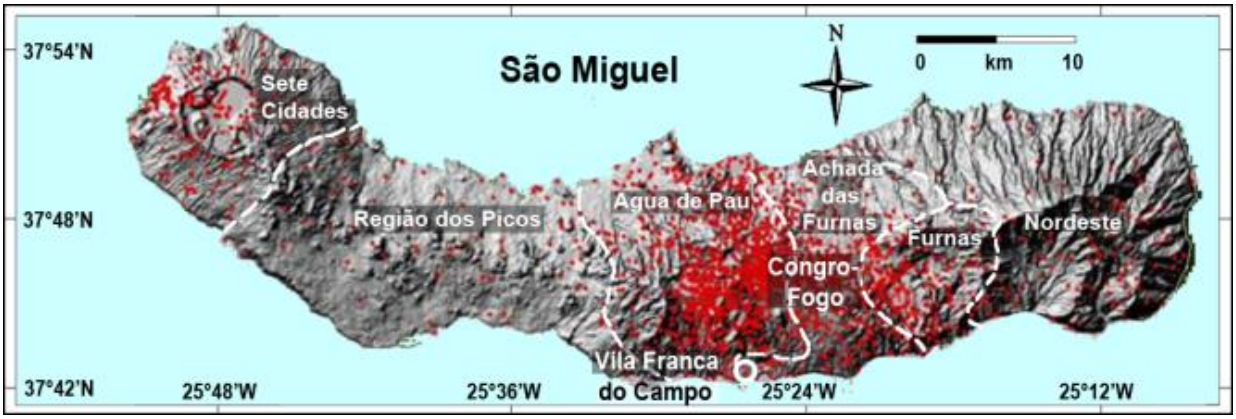

Fig. 4. *The epicentre distribution of earthquakes in São Miguel between 1986 and 2006. Vila Franca do Campo is marked with a white circle. The image is modified from Gomes (2006).*

volcanic eruption at Furnas, which could cause landslides possibly isolating the communities in the Furnas area (Guest et al., 1999).

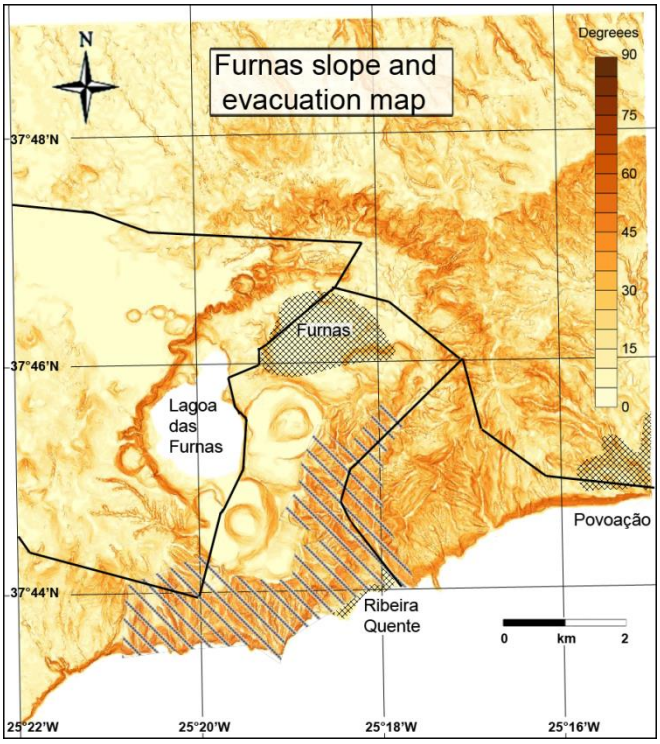

Fig. 5. *Slope map of the terrain of the Furnas area and the evacuation roads. The cross-hatched areas are populated and the stripes shows an area that is particularly at risk for landslides in Furnas and São Miguel (Valadão et al., 1999).*

1.3.3 Flooding

The water recharge area of the Furnas caldera measures ca. 33.2 km^2 and feeds the streams of Ribeira dos Tambores, Ribeira Amarela from Lagoa das Furnas and Ribeira Quente (Cruz et al., 1999). The outflow from Lagoa das Furnas basin passes Furnas village and ends at Ribeira Quente at the south shore. The water content in Lagoa das Furnas is ca. 13,000,000 m^3. A small barrier, ca. 7.4 m above the Lagoa das Furnas water surface, separates the lake from the valley that leads to Furnas Village. This barrier could breach due to an earthquake or a landslide without seismic activity if the soil is saturated and cause serious flooding in Furnas village and Ribeira Quente (Guest et al., 1999).

1.4 Two historical eruptions in Furnas volcano

When the first settlers discovered the archipelago of the Azores in the early 15th century, Santa Maria was the first island to be inhabited by the Portuguese during the autumn of 1431 (Guest et al., 1999). São Miguel was sighted from Santa Maria and an expedition was sent to the island in order to release animals for grazing. Sometime between 1439 and 1443 they returned to São Miguel and were met by ”tongues of fires” and earth tremors (Dias, 1936). A priest entered the valley and saw vapour rising and three lakes, later named Lagoa Grande, Lagoa Berrenta and Lagoa Obscura. Most likely, the described eruption corresponds to the latest eruption from Gaspar Dome (Guest et al., 1999).

The most recent eruption in Furnas is from 1630 and caused about 195 casualties. It was an explosive eruption of subplinian character with a dome building ending phase, described in detail by Cole (1995). At the time of the 1630 eruption, people were living in the Furnas valley and at the northern and southern coast of Furnas. The villages nearest to the caldera were Povoação, Ribeira Grande, Ponta da Garça and Vila Franca located at the southern shore (Fig. 6). Several first-hand observations from the

eruptions have been recorded. Manoel da Purificação describes “clouds of fire from two of the lakes” and violent tremors on Monday the 2nd of September 1630 between 8 pm and approximately 10 pm. He described a short time of calmness after the tremors and around 11pm an explosion blew away an “elevation” between two lakes (Fig. 6). That was the start of the latest eruption in Furnas where ashes from the eruption “turned the day to night” for the next three days (Da Purificação, 1880).

The narrative of Pedro da Ponte confirms the

Fig. 6. *On the left a map of the surroundings of Furnas volcano modified from Wallenstein et al. (2007). On the right a painting of the eruption in Lagoa das Furnas by Manuel Carreiro with direction from Victor-Hugo Forjaz.*

witnessing of tremors and a subsequent eruption on the night between the 2nd and 3rd of September, which was ongoing until Friday the 5th (Da Ponte, 1880). Moreover, Pedro da Ponte writes that 75 people died when they harvested “baga de louro” in the fields. Another witness, João Gonçalves Homem, describes three explosive active days with ash fall and a new eruption phase with tremors that “felt like the whole island was in swale” (Gonçalves, 1880). These tremors were ongoing for about two months. The consequences for the villages in the valley and south of Furnas were devastating, in Povoação only one functional house remained and in Ponta da Garça one house and one chapel was left. João Gonçalves Homem also states that 115 died from a pyroclastic surge in Ponta da Garça (Gonçalves, 1880). Furthermore, he describes that “the eruption consumed and dried two lakes” and that “Lagoa Grande continued to have clear water”. He also describes in detail “boiling water with smoke and fires” and “material spreads from three gaps“ on the south flank near the shore.

It seems likely that the reported Lagoa Grande in fact is the present Lagoa das Furnas and Lagoa Barrenta and Lagoa Obscura were the lakes in the valley that was lost due to the eruption. This is further described in more detail in the manuscript. Moreover, basaltic eruptions are restricted to the flanks of the volcano and basaltic dykes are exposed along the coast and form

offshore basaltic reefs (Guest et al., 1999). The gaps, described by João Gonçalves Homem, were most likely dykes with lava flows on the flank of Furnas volcano.

1.5 Earlier geophysical studies in crater lakes

Sub-bottom sonars are needed for penetrating the sediment stratigraphy and sidescan sonar (SSS) for making a mosaic of the sub-bottom. But, crater lakes are often located in remote areas and can be difficult to access. Nevertheless, several geophysical studies have been made and listed by Newhall et al. (1987). They list only 14 crater lakes where seismic reflection studies have been undertaken between 1971 and 1986. For example a geophysical and geological survey was made by Poppe et. al., (1985) in Laguna de Ayarza in Guatemala. This caldera lake is similar to Lagoa das Furnas in that it is a twin lake, but differs in that it is double the size. Powerful airgun sonar penetrated the sediment stratigraphy at least 170 m revealing a chaotic caldera collapse. Even though the geophysical study was made by airgun sonar the signal was attenuated by gas in some areas in the lake. An airgun sonar together with a sidescan sonar were used for making an image of the lake floor and for collecting sub-bottom profiles in Crater Lake, Oregon (Nelson et al., 1986).

Moreover, more modern multibeam sonars have the capability to acquire both high resolution mosaics of lake floors and high resolution sub-bottom profiles. The survey on Crater Lake (Oregon) 2002 was likely one of the first surveys with multibeam technique in a crater lake (Bacon et al., 2002). They revealed landforms in striking detail and also new features were discovered. Lake Albano was investigated by multibeam bathymetric survey in 2005 which provided e.g. detailed 3-D maps and information of earlier unknown morphological features (Anzidei et al., 2006).

2 Methods

2.1 Geophysical mapping

In November 2012 a geophysical survey was conducted of Lagoa das Furnas using a sidescan sonar and single beam echo sounder. The survey was complemented by sediment coring, drilling and visual bottom inspection by divers. A small vessel (~ 1.5 m x 4 m) was used to accomplish both the geophysical mapping and the sediment coring (Fig. 7). This description of applied methods complements that of the manuscript by adding addition technical details and the fundamentals of the used mapping and coring techniques.

2.1.1 Acoustic mapping methods

A single beam echo sounder was used for bathymetric data and to acquire sub-bottom profiles. Echo sounders are capable of penetrating the sub-bottom sediment stratigraphy. The penetration is a result of

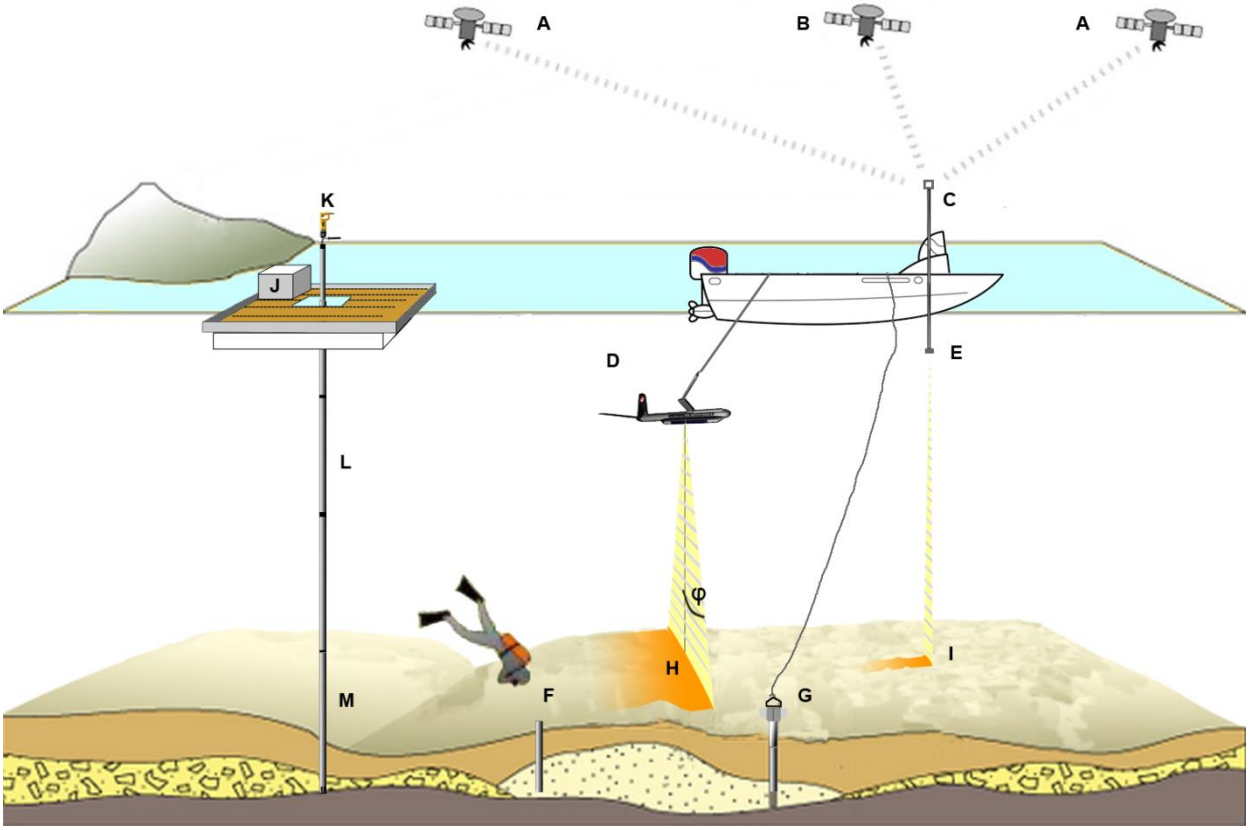

Fig. 7. *The image shows an illustration of the sampling methods in Lagoa das Furnas. Modified from SGU, The Geological Survey of Sweden, http://www.sgu.se/om-sgu/verksamhet/kartlaggning/maringeologisk-kartlaggning/utrustning-for-kartlaggning-av-havsbottnen/. A (GPS satellite),B (geostationary satellite for SBAS correction) and C (Hemisphere 100 GPS antenna) show the SBAS GPS-system. D (sidescan sonar) and E (single beam sonar) are acoustic sonars used to map the lake floor and uppermost sub-bottom sediment stratigraphy (H, I). The maximum opening angle, φ, applied for the sidescan sonar swath is shown. F shows a diver penetrating the lake floor with plastic pipe and G is a portable gravity sampler. K shows the handheld drill machine with electrical generator (J), L and M show the drill rods and core barrel, respectively.*

the used frequency of the sound lobe and acoustic characteristics of the geologic material. The reflected signal is proportional to the amplitude from the transducer and the magnitude of the acoustic impedance contrast. Acoustic impedance contrasts within the sediment stratigraphy will give rise to reflections of the transmitted sound lobe, which continues to propagate through the sub-bottom stratigraphy until it has lost all its energy. The sound lobe will lose energy before reaching the sub-bottom material, when traveling through the water column mainly through acoustic absorption. The pressure amplitude will be absorbed depending on the two-way distance and the frequency of the sound lobe approximately by:
(The following theory is mainly based on synopsis on signal theory provided by Mosher and Simpkin (1999). While the presented equations are from standard acoustic theory, they are here presented in the forms given by Mosher and Simpkin.)

$$P_r = \frac{P_0 e^{-\alpha_k f_r}}{r} \qquad (1)$$

where P_r is the pressure amplitude received from the source amplitude, P_0 at a distance r. α_k is the absorption coefficient and f_r is the frequency of the sound lobe. From this equation it is clearly seen that longer distances from the acoustic source as well as higher applied frequencies will yield lower pressure, resulting in weaker echoes from targets. Large acoustic characteristic impedance contrasts between subsequent geological layers imply stronger echoes. Seismic reflection is the reflection of a sound lobe between two media with different impedance and the size of seismic reflection is determined by:

$$\mu_0 = \frac{I_2 - I_1}{I_2 + I_1} = \frac{V_2\rho_2 - V_1\rho_1}{V_2\rho_2 + V_1\rho_1} \qquad (2)$$

where μ_0 is the reflection coefficient, I is the acoustic impedance, V is the compressional sound speed and ρ the bulk density. The first strong echoed signal is usually representing the sea/lake bottom since there is commonly a large acoustic characteristic impedance contrast between the water and bottom material. Moreover, geologic characteristics of the lake floor will influence the size of the seismic reflection. A rough lake floor will scatter the sound lobes and reduce the echoed signals more than a flat lake floor. Slope angles of the bathymetry will also reduce the strength. A high incidence angle (Fig. 7) of the beam will decrease the size of the returned signal and is normally compensated for in the post processing of the acoustic data. The reflection coefficient μ_0 is therefore reduced by:

$$\mu = \mu_0 \exp -(\frac{4\pi h sin\varphi}{\lambda})^2 = \mu_0 e^{-R^2} \qquad (3)$$

where μ is the reduced reflection coefficient, h is the depth, φ is the incidence angle and λ is the wave length of the sound lobe. R is called the Rayleigh coefficient and describes the size of scattering. Wave length λ is based on the frequency (f) and the velocity (V) of the sound lobe according to:

$$V = f \times \lambda \qquad (4)$$

The vertical resolution, R, of the received signals is often estimated to about $\lambda/4$ and is called Rayleigh Criterion.

$$R = \frac{V}{4f} \qquad (5)$$

This means that the physics of sonars with near singular high frequency of the sound lobe is capable of providing a higher resolution (Equation 5) portrayal of the sub-bottom stratigraphy but the signal will on the other hand attenuate (Equation 1) and scatter more (Equation 3). Consequently, low

frequency lobes will penetrate more, though, with a lower resolution. To overcome this dilemma another type of sonar can be used. Chirp sonar produces a signal which sweeps from a lower to a higher frequency in a pulse. The difference between the higher and the lower frequency is called the bandwidth. The frequency range is anywhere between 400 Hz and 20 kHz. The resolution, R, of a chirp is decided by (Schock et al., 1989):

$$R = \frac{V}{2B} \quad (6)$$

where V is the sound velocity and B is the bandwidth. This type of sonar yields a higher resolution and a deeper penetration compared to sonars with constant frequency.

The sidescan sonar emits fan shaped beams downwards and to the sides and is towed behind the boat and is sometimes called a "towfish" (Fig. 7). The frequency used in sidescan sonar is high, generally between 50 kHz to 1,000 kHz which results in high attenuation in the water column and limited penetration in the sub-bottom. Earlier models printed out the mosaic directly on scrolling papers but since the late 1980s the computer has been able to process sidescan data and e.g. correct towfish instability (Oppenheim and Cobra, 1988). The returned echoes to the transducer in sidescan sonars are sometimes called backscatter and will be in this paper. Sidescan sonar is used to get a high resolution picture of the lake/sea floor and to identify objects on the lake/sea floor e.g. Lee and Kim (2004). It is also used for classification of the top sediment on the lake floor, called acoustic seabed classification, e.g. Collier and Brown (2005).

2.1.2 MD 500 single beam echo sounder

We used a portable 28 KHz Meridata MD 500 hydrographic echo sounder for bathymetric data and to acquire sub-bottom profiles (Fig. 7). The 28 kHz transducer of this high frequency sub-bottom profiler was mounted on an aluminium pole attached to the starboard side of the boat. The pole was mounted vertically in order to point the transducer with an angle of 0° towards the lake bottom. In order to achieve accurate depths, a sound velocity probe was used to measure sound velocity profiles of the lake water at stations spread out over the survey area. From these stations, a harmonic mean

Fig. 8. *Boat and the sidescan sonar (A) with the computers receiving the sub-bottom and sidescan sonar backscatter data (B).*

of 1471 m/s was calculated. This value was taken to be generally representative of the surveyed part of the lake and applied when converting echo sound travel times to depth.

2.1.3 Klein 3000 sidescan sonar

A Klein 3000 dual high frequency (100/500 kHz) sidescan sonar was used to map the surface of the lake floor (Fig. 7). The sidescan towfish was towed behind the boat to minimise noise disturbance from the outboard motor. The high frequency of the sonar generates and receives high resolution data for detection of small targets. The sidescan sonar has a fan shaped beam that covers a large area of the lake floor. Maximum incidence angle is 40° and the towfish can also be tilted between 5° to 25°. The disadvantage of high frequency sonars is high attenuation in the water column but Lagoa das Furnas Lake is shallow with a maximum depth of ca. 11 m and the attenuation is relatively low.

2.1.4 Hemisphere 100 GPS

Navigation was provided by mounting a Hemisphere 100 GPS smart antenna on the upper end of the pole where the MD 500 transducer was mounted (Fig. 7). This gives a minimum offset between the GPS positions and the echo sounder transducer, which helps to minimise navigational errors. The satellite-based augmentation system (SBAS) was used to enhance the navigational accuracy. SBAS uses geostationary satellites (Fig. 7) and yields a horizontal accuracy of approximately 2 m. The positions provided by the Hemisphere 100 were also used for the sidescan mapping.

2.1.5 Software

The software of the MD 500 MDCS server, the core of the system, enables other programs to communicate with each other e.g. compass, motion sensor (compensation for heave and tide), sound velocity profiler and the MD 500 Echo Sounder. With two computers it was possible to use both the single beam sonar and the sidescan sonar at the same time (Fig. 8). To get absolute positions MD receives real-time GPS positions.

The SSS mosaic and sub-bottom profiles were post-processed with Chesapeake's SonarWiz 5 (Fig. 9). The SSS mosaic was adjusted with several methods for image enhancement. One important method was the "Automatic Gain Control" (AGC), used for compensating data loss for high beam

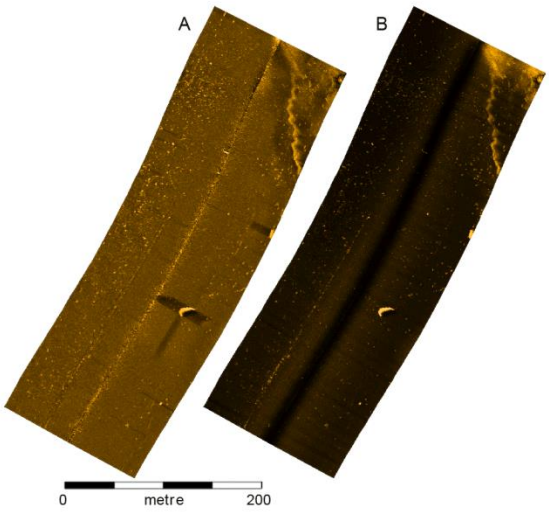

Fig. 9. *A is a processed sidescan mosaic in SonarWiz and B a non-processed mosaic.*

incident angle that will reduce the acoustic return. Figure 9 shows a non-processed sidescan mosaic lane before and after adjustments of the returned acoustic signal. The black stripe in between the port and starboard swaps is the nadir, and represents the water column. The AGC was also used for sub-bottom profiles for compensation of energy loss when the signal penetrates the water column and the sediment. An example of single beam mosaic is shown in figure 14 and figure 17.

The depth data from the single beam sonar was exported for further gridding. Digital Terrain models (DTM) were generated by Surfer 10.7.972 and gridded with the Kriging interpolation algorithm with 10 m spatial resolution. That algorithm works well for interpolation in areas of sparse data (Oliver and Webster, 1990). 2-D maps were made by Surfer and the 3-d processing was carried out with Global Mapper 15.0.6 and Fledermaus suite 7.3. Garmin GPSMAP 60CSx Handheld GPS Navigator was used to mark samples and Lagoa das Furnas shoreline. EasyGPS 4.79 was used for import of the coordinates and Earthpoint for conversion coordinates.

2.1.6 Geodetic datum and projections

Given that the earth is flattened at the poles and composed of varied topography the following steps were taken for the mapping of Lagoa das Furnas and the Furnas area. The World Geodetic System 1984 (WGS 84) reference surface was employed, a standard

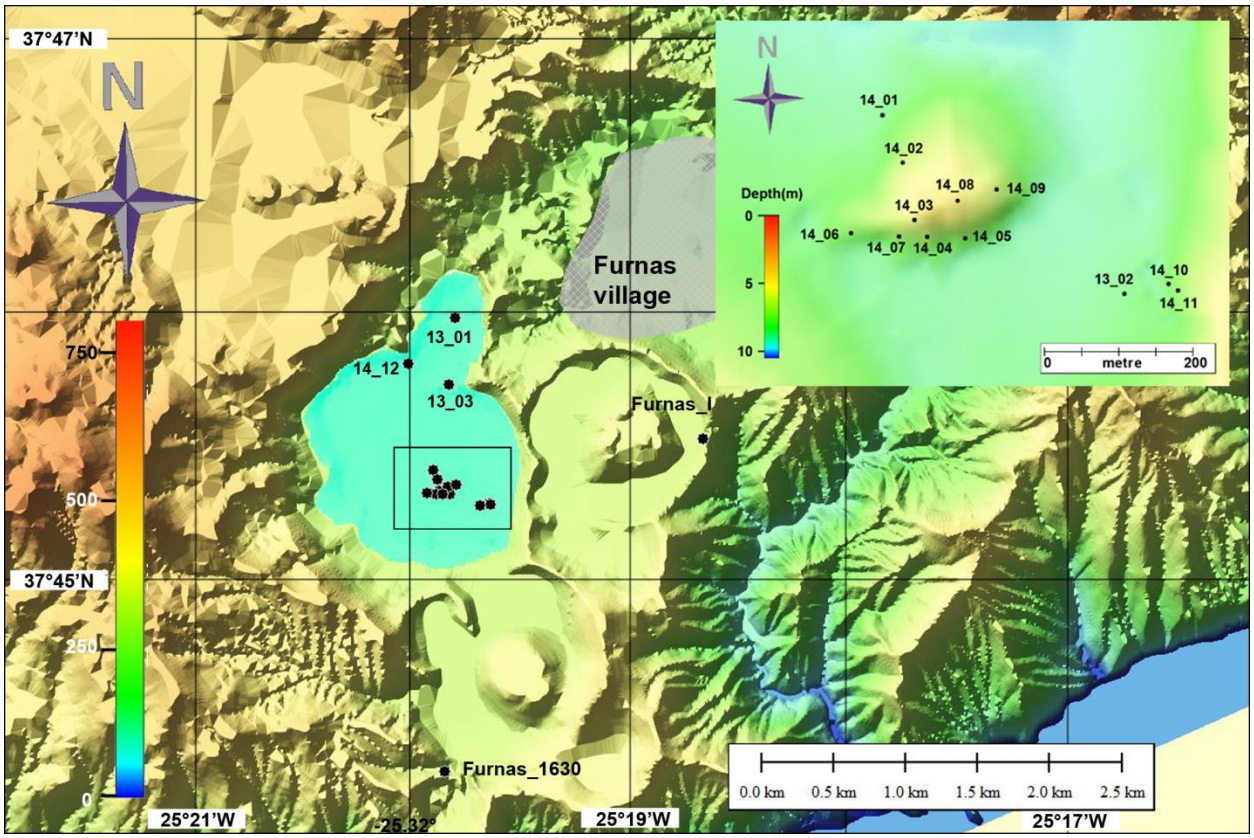

Fig. 10. *Sampling map from the lake floor and land. The inset show sample sites from the cone (14_01-14_09), from an area with high acoustic return (14_10-11) and from a layer visible from the sub-bottom stratigraphy (13_02). DTM and the inset bathymetry were generated with GlobalMapper.*

system used in cartography. All topological maps, bathymetric maps and sidescan sonar mosaics were overlain in Universal Transverse Mercator (UTM) projection. UTM projection covers the reference surface in 60 conformal zones; the Azores is located in Zone 26N.

2.2 Sediment coring and drilling

Sediment cores were retrieved from the lake floor of Lagoa das Furnas in June 2013 and May 2014. Selection of the sample stations in the lake was based on the earlier geophysical survey.

In total 12 sediment cores were collected in 50 mm plastic pipes by divers pressing and hammering the pipes into the lake bottom (Fig. 7). Dredge samples were collected from two sites in the lake. One was collected at position 14_03 at a depth of ca. 1.3 m and the other, 13_03 on the ridge between the northern and the southern part of the lake (Fig. 10). Also, three samples (14_10, -14_12) were collected by a specially designed portable gravity sampler, see 2.2.1. In addition, lake floor samples were obtained by drilling in May 2014. This was carried out with an Atlas Copco 1500 mm conventional single tube core barrel (Fig. 7). The diameter of the corer was 46 mm and the recovered cores were 32 mm in diameter. The corer was connected to a drilling machine by drill rods produced by Atlas Copco that were designed for drilling in water depths up to 4.5 m. To increase this depth limit, additional 6 m drill rods were constructed from 27 mm steel pipes. The drilling machine was handheld and powered by an electrical generator driven by gasoline. Drilling was undertaken from a 3 x 4 m anchored platform. Finally, samples were taken on land from eruptive sites of the two most recent Furnas eruptions: Furnas I and Furnas 1630 (Fig. 10).

2.2.1 Portable core sampler

In order to collect sediment samples without divers, a portable core sampler for loose lake sediment was needed. This corer was designed to be portable and to cause minimum disturbance of loose lake sediments. The total weight of the sampler is 12 kg with material of steel and PVC (Fig. 11).

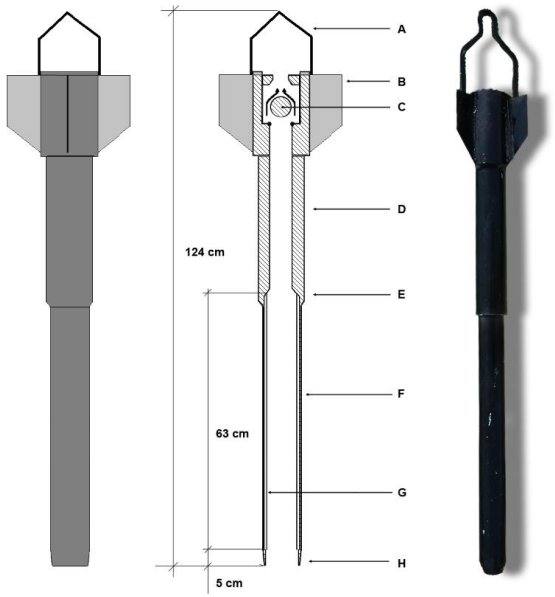

Fig. 11. *Portable core sampler for loose sediment.*

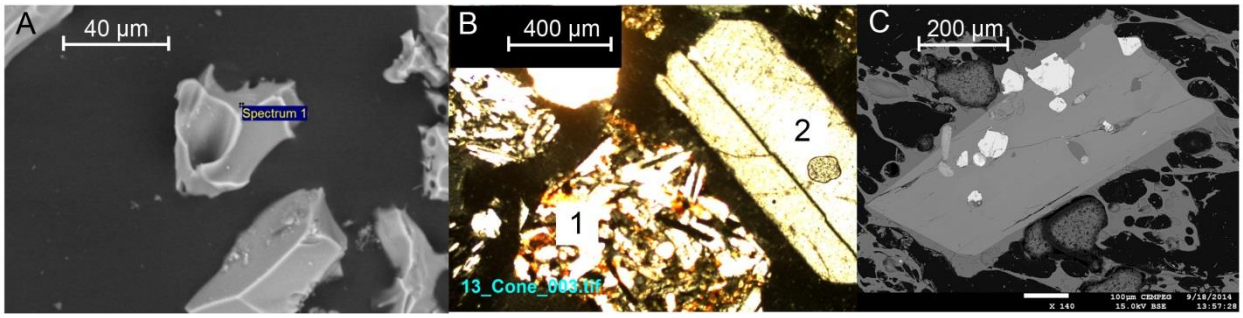

Fig. 12. *Scanning electron micrograph of tephra from the cone in Lagoa das Furnas with characteristic tephra morphology with bubble wall (Lowe, 2011) in (A) and photomicrograph minerals from petrographic microscope in B. (1) shows trachytic matrix, and (2) the most common phenocryst, feldspar. C is a backscatter electron image of feldspar from the electron microscope in Uppsala University.*

To maintain stability, two wings were welded on the top of the corer (B). The check valve (C) lets the water flow through the sampler on the way down to the lake floor. This will minimise the bow wave in front of the sampler which can disrupt the sediment when the sampler hits the lake floor. This is a common design feature for samplers of loose sediment (Blomqvist, 1991). The check valve is mounted with a screwed cap on the top. Further down the corer has an inner diameter of 40 mm and outer diameter of 70 mm (D) that ends with a thread (E). An outer steel thread cylinder (F) holds the 50 mm plastic pipe (G) with a length of 630 mm. The corer edge is sharp for best penetration in the sediment (H).

For operation, the corer needs to be complemented with plastic tape around the attachment (E) to ensure it will hold under pressure. A rope attached to the holder (A) and the corer is lowered into the water and released. After penetration the sampler is retrieved to the surface. During withdrawal, the check valve will close and the under-pressure will hold the sediment in the plastic tube.

2.3 Rock sampling and geochemical/petrological analysis

Three sediment cores were analysed with a non-destructive multi-sensor core logger (MSCL) and nine cores were scanned with ITRAX X-ray fluorescence (XRF) at the Department of Geological Sciences, Stockholm University (SU). After the non-destructive analyses the cores were described lithologically. Detailed core descriptions are presented in the manuscript. Furthermore, sub-samples of tephra were sorted out from the lake cores and from the land-based Furnas I and Furnas 1630 eruptive sites. The tephra was pulverised to a size between 40 µm to 150 µm in a mortar and mounted on stubs (Fig. 12). These samples were analysed for 13 major elements using a scanning microscope Philips XL-30 with an energy-dispersive spectrometry (EDS) at SU. In addition, twenty 0.03 mm thin sections were prepared at SU and Vancouver Petrographic, Canada. Seven of these thin sections were analysed using a JXA-8530F electron microprobe

analyser with wavelength-dispersive spectrometers (WDS) at the Department of Earth Sciences, Uppsala University (Fig. 12). This is a common method for tephra analyses (Lowe, 2011). Volcanic glass and minerals from the thin sections were also studied using a petrographic microscope and modal estimates were carried out at SU (Fig. 12). Radiocarbon dates were obtained from three samples at the Department of Geological Sciences at Lund University.

3 Results

3.1 Backscatter and acoustic returns analysis

The sub-bottom profiles show a maximum penetration depth of ca. 3 m with the single beam sonar (Fig. 14). A possible reason of this limited penetration of the acoustic signal is gas content and micro bubbles in the sediment that attenuate the seismic waves (Fonseca et al., 2002, Hovland and Judd, 1988). Gas in the sediment can be methane from decomposing plants and/or carbon dioxide from volcanic activity (Fig. 13). Moreover, undulations, pockmarks and a small layer of decomposing organic material were omnipresent on the lake floor and probably scattered the sound lobe and reduced the reflected signal (Fig. 13).

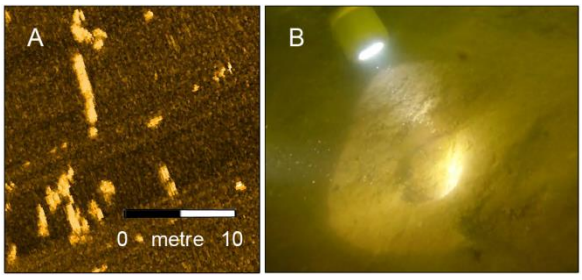

***Fig. 13**. Seepages from a western part of the lake floor (A) and pockmark on the cone from the underwater camera (B).*

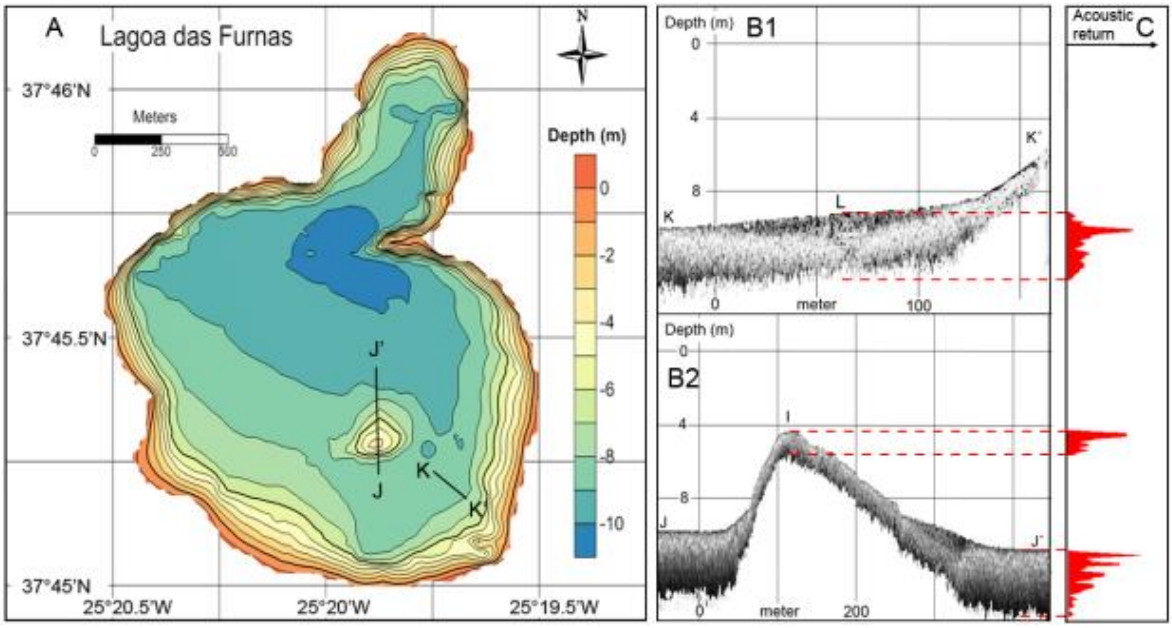

***Fig. 14.** Bathymetry of Lagoa das Furnas made from seismic data. The grid was generated by linear Kriging interpolation of 10 m spatial resolution (A). Two cross sections one of the loose sediment area K – K' (A) and the other intersects the cone (J – J'). B1and B2 show the seismic reflections from K – K' and J – J' respectively, lighter mosaic means stronger acoustic signal return. The acoustic reflections from three representative pings from each area are shown in C from the marked area in B1 and B2.*

3.1.1 Single beam sonar

Figure 14 shows the bathymetry map made by Surfer with depth data from the single beam sonar. As mentioned in section 3.1, the penetration depth was limited. Figure 14 also shows the three recognizable categories of acoustic returns from the single beam sonar. The choice of the specific return signals in figure 14 was based on the typical features of the ping signals for each category. At J' on B2 in figure 13 shows the dominant acoustic return characteristic from the lake. The first acoustic return shows a relatively slow increased signal strength that probably comes from the small layer of decomposing organic material, as described above. The signal peaks when it encounters gyttja clay, with an organic content of ca. 6 %, and thereafter gradually decreases and terminates at ca. 3 m. (The sediment depth is based on the water velocity, 1471 m/s, which will result in an underestimated value.) On the cone, the signal encounters harder lake floor such lapilli, coarse ash and compacted ash (Fig. 14). The penetration of the cone was ca. 1 m. The attenuation pattern is similar as with clay gyttja but shorter.

At the eastern part of the lake (the transect K-K' in figure 14), we were able to establish a relative distinct stratigraphy. The uppermost layer held a higher content of organic material, ca. 9 %, and the water content was also higher. The signal penetrates this softer material ca. 1 m and subsequently encounters another layer with different impedance and reaches the maximal acoustic return. From there the signal decreases gradually (B1 in figure 14).

3.1.2 Sidescan sonar

A covering sidescan sonar mosaic from Lagoa das Furnas is shown in figure 6 in the manuscript.

Ground-truthing of the lake floor was made by analysis of sediment cores and underwater films from a GoPro Hero video underwater camera. The reason for ground-truthing is to make an acoustic seabed classification (ASC) by studies of the

Site	Description	Classification
A, B	Deep parts of the lake.	Gyttja clay
C	Totally 9 samples on the cone. The finest material was found on the flanks.	Fine material Coarse material Gyttja clay
D, E	Two samples on an area with high back-scatter (D) and one on the rim (E).	Coarse material
F	Area with hydro-thermal deposits.	Fine material

Table 1. *Ground-truth classification data.*

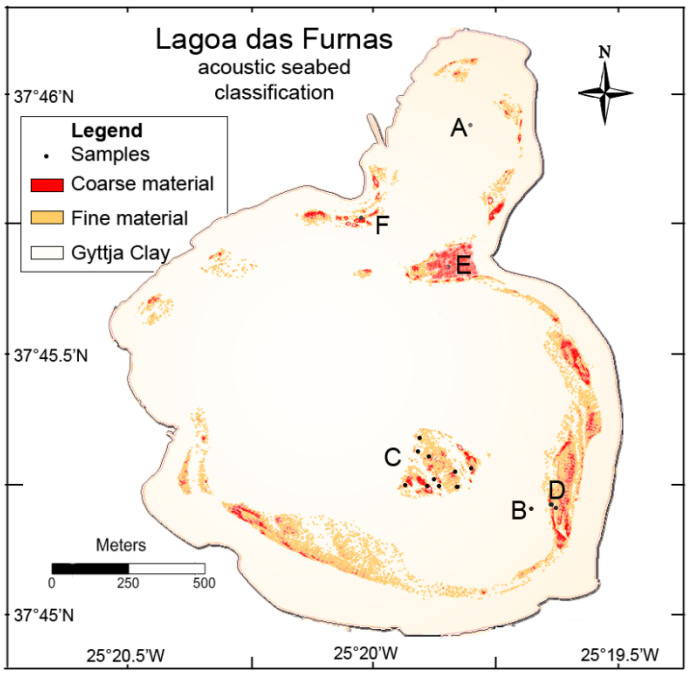

Fig. 15. *Seabed classification map based on SonarWiz´s Seabed Classification and correlated to ground-truth data.*

correlation between the features of the sediment and the characteristic of the backscatter (Anderson et al., 2008). In short, a strong signal is assumed to indicate hard lake floor and a weak signal is assumed to indicate soft lake floor which absorbs the signal more (Bellec et al., 2008). The Seabed Classification manager in the computer program SonarWiz was used to classify different textures in the sidescan sonar mosaic. The program uses a square window and several statistical calculations for every pixel in the image. The square could be, for example, the eight nearest neighbours of a pixel. One useful statistical process calculated the standard deviation of the pixels in the window which resulted in a "smoother" image. Before the classification process, the program was "trained" on representative mosaic lane(s) to identify a number of different textures. Each pixel in figure 15 was calculated from 24 neighbours and the result was divided into six different classes with unique colours. This seabed classification was then correlated with the samples from the lake and reduced to three classes in Photoshop (Table 1 and Fig. 15).

3.2 Debris from mass movements

In the western part of the lake, the caldera wall is steep and affected by landslides (Valadão et al., 1999). Larger landslides have created lobes of debris on the lake floor. The largest landslide in the lake was found in the western part of the lake near the steep caldera wall (Fig. 16). Calculation of the mass movement volume was made with a method with two gridded maps (Völker, 2010) (Fig. 16). One additional grid was made with the depth contour lines of the landslide repositioned to the same slope contours adjacent to the landslide. The difference between the two volumes was about 10,000 m^3.

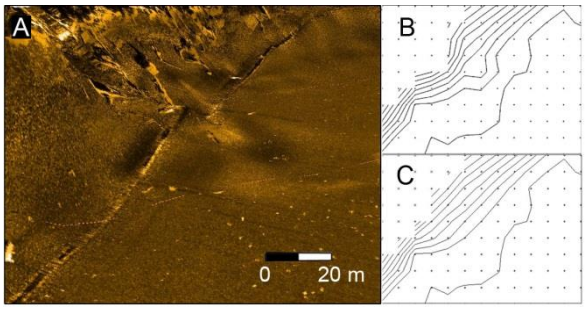

Fig. 16. *3D mosaic view of the largest landslide from south and exaggerated 6 times (A). B is the original grid with the landslide and C the grid with the landslide removed.*

In addition, the loose sediment with increased organic content was measured (Figs. 14 and 17). The outreach of the sediment was profiled in SonarWiz from the sub-bottom profiles. A new bottom profile was made with the sediment removed and exported to Surfer and gridded with kriging using the same method as the original grid. The volume of the sediment, 45,000 m^3, was calculated from the difference between the grid from original lake and the grid from the lake with outreached lake floor.

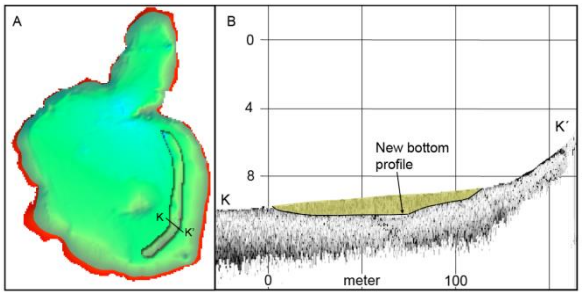

Fig. 17. *Sub-bottom profile record along K-K' (A) shown in figure 13. The marked area in B contained clay gyttja with high water content.*

3.3 Summary of manuscript

This manuscript presents results from geophysical mapping of Lagoa das Furnas and sedimentological, petrological, geochemical and geochronological studies of sediments samples from the lake floor. Based on bottom characterization of Lagoa das Furnas, a newly discovered volcanic cone on the lake floor is described and proposed to be linked to one of the volcanic eruptions that took place in 1630. The origin of the cone is supported by a correlation between tephra deposited on the cone and tephra from the Furnas 1630 and Furnas I eruptions.

Based on a compiled bathymetric map and a sidescan mosaic assembled from data acquired in this study, the overall morphology of the lake floor is described and geological features such as hydrothermal deposits, seepages and pockmarks are located. Furthermore, debris lobes from mass movements were found in the western part of the lake just below the steep caldera rim (Fig. 18).

The most prominent mapped feature in the lake floor is clearly expressed by a different backscatter signal. This bathymetric height, located in the southern part of the lake, takes the form of a circular oblique cone (Fig. 19). The cone rises ~5 m above the lake floor and has a basal diameter of ~300 m. Its volume is approximately 100,000 m^3 and the slope angle of it sides is between 2° and 5°.The surface texture of the cone is coarse with small pockmark-looking depressions and small winding fissures.

To investigate the nature of this cone, nine sediment cores were acquired along two transects across the cone (Fig. 19). In order to unravel the origin of the cone, samples were taken from the two most recent eruptions, Furnas I and Furnas 1630. The lithostratigraphy, geochemistry and mineralogy of these cores were studied in this work.

The sediment cores retrieved from the cone are comprised of pyroclastic debris with alternating layers of ash, pumice and lapilli indicating explosive subaqueous eruptions. The spatial distribution of pyroclastic debris in the area of the cone is consistent with the hypothesis that the debris were produced from eruptions of the cone itself rather than being draped over the cone by an eruption

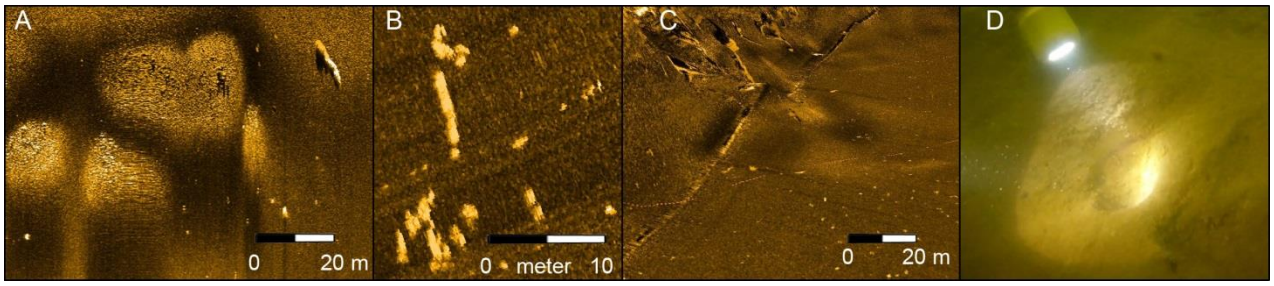

Fig. 18. *Sidescan sonar mosaic of the lake shows: hydrothermal deposit (A), an area with high gas seepages activity (B) and mass movement material (C). Small funnel shaped pockmarks were frequently on the lake floor, here documented with a GoPro underwater camera on the cone (D).*

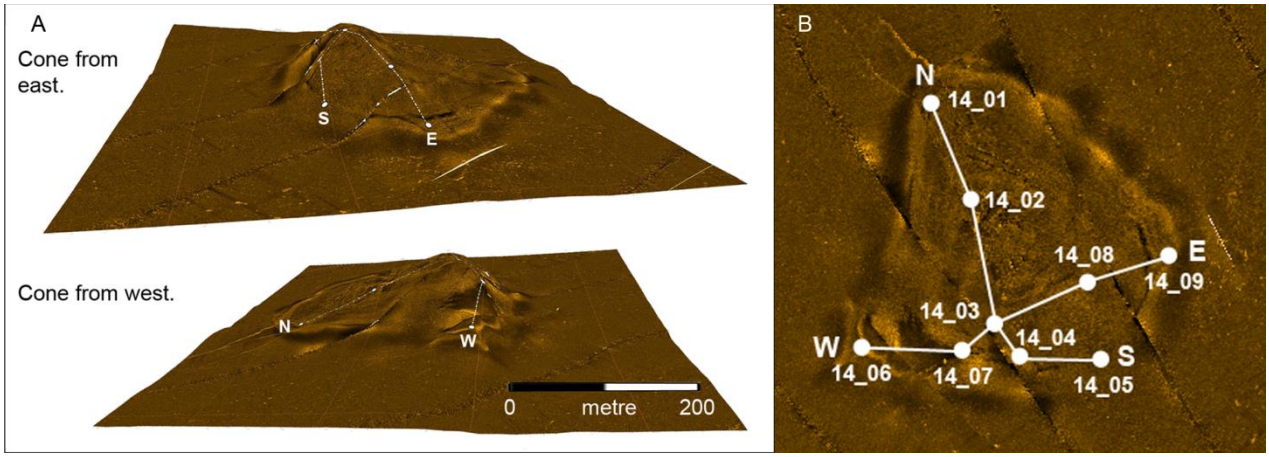

Fig. 19. *The southern part of the lake is dominated by a volcanic cone (A); the illumination is from north and the picture is 20 times vertically exaggerated. Two transects (No-So;We-Ea) are marked on the cone with nine samples marked 01-09 (B). Higher backscatter intensity was found on the base of the cone.*

located elsewhere. Result of drilling on the cone indicates blocks or bedrock below 1.3 m of pyroclastic debris.

^{14}C-dating reveals that the cone most likely was formed during the Furnas 1630 eruption. Geochemical, petrological and statistical studies of the pyroclastic material confirm that it belongs to the same magma series as the 1630 eruption. The chemical components of all analysed tephra show strong intermutual similarities. Applying Borchardt's coefficient table gives a maximum difference of 4 % for major elements and Ward's minimum variance method distinguishes two major groups with maximum dissimilarity, one with tephra from Furnas 1630 and Furnas I and the other containing all samples from the cone. The silica content of pyroclastic debris from the cone suggests a more evolved magma than Furnas 1630, with an increased content of phenocrysts, dominated by feldspar. This suggests that during a late phase of Furnas 1630 eruption phase Lagoa das Furnas erupted and a dome or a block-and-ash-cone in the southern part of the lake was formed.

4 Discussion and conclusions

The high-resolution sidescan mosaic assembled in this study shows that the lake floor of Lagoa das Furnas is scattered with gas seepages and that there are two areas with hydrothermal deposits. Moreover, pictures from an underwater camera and reports from divers revealed pockmarks on the mapped cone in the southern part of the lake as well as in all other parts of the lake. The single beam sonar was used to characterise the uppermost metres of accumulated sediments and for acquiring depth data of the lake. In total, 35 km of survey lines were acquired in the lake, which was adequate to generate a general view of the lake bathymetry and characterise the uppermost bottom sediments. By draping the mosaic onto the bathymetry, the volcanic cone mapped in the southern part of the lake

is clearly visible. In the manuscript, the eruption producing the cone is suggested to come from a late stage of the Furnas 1630 eruption. These results as well as the methods producing them are here further discussed.

The sub-bottom penetration achieved using the 28 kHz MD 500 in the relatively shallow Lagoa das Furnas did not exceed ~3 m (see chapter 3.1). Previous mapping with this particular sonar has generally provided much better results. For example, during surveys in Lake Vättern, southern Sweden, the penetration was approaching 15 m in 100 m water depth and apparently similar bottom sediments with respect to grain size as in Lagoa das Furnas (Personal communication, Martin Jakobsson, SU). Other studies of crater lakes using more powerful sonars with lower frequencies have shown good results with respect to sub-bottom penetration (e.g.

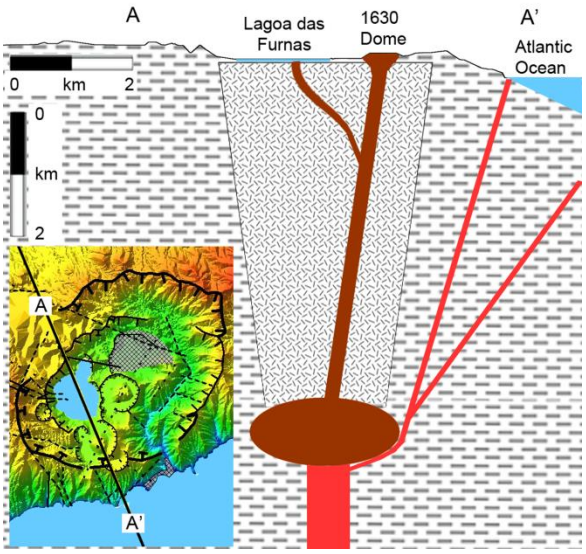

Fig. 20. *The inset shows the cross section of Furnas volcano. The magma chamber is presumed to be located at a depth of ca. 5 km (Blanco et al., 1997). The horizontal and vertical scales of the map are equal.*

Poppe et al., 1985). However, it is also noted in previous studies that crater lakes may have large amounts of gas in the sediment (Poppe et al., 1985, Newhall et al., 1987), which causes a known problem for sub-bottom profilers (Mosher and Simpkin 1999). Gas will scatter the acoustic signal and absorb the energy. The abundant small pockmarks and mapped areas of hydrothermal vents in Lagoa das Furnas suggest the presence of gas. This may explain the poor performance of the 28 kHz MD 500.

During the last 5,000 years there is no evidence of basaltic intra caldera. This might depend on the inability of basaltic magma to enter the magma chamber (Booth et al., 1978). The absence of basaltic eruptions in the caldera indicates a large trachytic magma chamber compared to it relatively small size of the volcano (Moore, 1991b) (Fig. 20). During this time as stated in e.g. Booth et al. (1978) “There is no evidence that basaltic eruptions took place anywhere on the volcano during this period”. Nevertheless, historical records from 1630 strongly indicate basaltic eruptions from the southern shore line of Furnas volcano (Gonçalves, 1880) (See 1.4).

Furthermore, injection of basaltic magma can trigger trachytic eruptions (Sparks and Sigurdsson, 1977) and silicic eruptions is often preceded by basaltic eruptions (Eichelberger and Gooley, 1977). Most likely were the possible basaltic eruptions on the shore, magma that was prevented from entering the magma chamber in an early stage of Furnas 1630 eruption phases. There are also strong indications of penetration of

basaltic magma during fractional crystallisation in the Furnas 1630 magma chamber (Rowland-Smith, 2007).

An interesting and important dimension of this research is the historical records. An early hypothesis was to connect the eruption from the cone to one of the lakes with "clouds of fires", described by Manoel da Purificação, see 1.4. However, our research points to an eruption in the third lake, Lagoa Grande, which most likely is the existing Lagoa das Furnas.

The geochronology established in this work suggests that this cone was produced sometime during the 1630 event. This chronology was far from simple to establish, in particular due to the large risk of contamination of the lake-floor sediment as well as plants growing near the lake by "old" carbon from the hydrothermal venting. Older carbon originating from the hydrothermal venting will influence any ^{14}C-dating on organic material in the sediments. This also showed in ^{14}C-dating of sediment samples from the northern shoreline (see manuscript chapter 4), which clearly yielded ages that was too old (Björck et al., 2006).

On the eastern part of the lake it is only a 7.4 m high barrier that prevents the water from Lagoa das Furnas from flooding the Furnas valley with its two villages downstream. This is an area with high risk concerning landslides and flooding (see section 1.3.2 and 1.3.2). To make a simulation of a barrier breach and following flood wave is an interesting and necessary research project. The western part of Lagoa das Furnas also faces a steep 200 m caldera wall of unconsolidated material. The conditions here are similar to those at Lake Tahoe, which is located in a tectonically active area framed by steep walls from where several landslides and debris flows have moved material into the lake. Detailed bathymetric mapping by Gardner et al.(2000) enabled volume calculation of mass moved debris into Lake Tahoe. The major landslide, named McKinney Bay Landslide, occurred between 21 and 12 ka (Moore et al., 2014). Moore et al. calculated the volume of this landslide to ~12 km^3 and made a simulation of the landslide and subsequent tsunami flood. The course of events of landslide and flood wave has also been animated by Ward (2001). A simulation of a landslide and subsequent flood wave in Lagoa das Furnas would determine whether if the wave would be able to wash away the barrier.

Acknowledgements

First I want to thank my supervisors Otto Hermelin and Martin Jakobsson. Both for the idea of the exciting research object and for all help in sample collections and writings. Also many thanks are directed to Alasdair Skelton for the geochemistry help and for making the text more readable. From the Department of Physical Geography, Stockholm University, I want to thank Stefan Wastegård for sharing wise tephra knowledge. From the Department of Geological Sciences, Stockholm University, I also want to thank; Hildred Crill for the writing help, Dan Zetterberg for his thin section work, Malin Kylander for Itrax analyses and Matt O´Regan for the MSCL analyse help, Marianne Ahlbom for ESEM analyse, Ines Jakobsson for interpretation of ancient Portuguese, Olivia Andersson for assisting with finding organic material, Josefin Linde for the point counting and Rickard Gyllencreutz for help with GIS problem.

I also want to thank Dr. Pacheco and Professor Gaspar at Centro de Vulcanologia e Avaliação de Riscos Geológicos, Universidade dos Açores, for the supply of the boat on Lagoa das Furnas and Jarek Majka at the Department of Earth Sciences, Uppsala University for assistance with micro probe analyses. Furthermore, the diver Johan Skantz, from the Department of Geological Sciences, Stockholm University, helped with sampling together with Johan Johansson from the University of Gothenburg. I also want to thank the local divers from the Azores, João Pedro Soares, Rui Patricio de Melo, Renato Verdadeiro and diver assistants. For help with drilling equipment and drilling advice I thank Anders Olsson and Ingemar Larsson. For the help with manufacturing of the portable sampler I send gratitudes to Bruksgymnasiet in Gimo.

I also want to thank Östhammars kommun and my principal Irmeli Bellander for their efforts that gave me the oppurtunity to join the Research school focusing on natural hazards. Finally I will thank my family for supporting me during this time.

References

ABDEL-MONEM, A., FERNANDEZ, L. & BOONE, G. 1975. K-Ar ages from the eastern Azores group (Santa Maria, São Miguel and the Formigas islands). *Lithos,* 8**,** 247-254.

ANDERSON, J. T., VAN HOLLIDAY, D., KLOSER, R., REID, D. G. & SIMARD, Y. 2008. Acoustic seabed classification: current practice and future directions. *ICES Journal of Marine Science: Journal du Conseil,* 65**,** 1004-1011.

ANZIDEI, M., ESPOSITO, A. & DE GIOSA, F. 2006. The dark side of the Albano crater lake.

BACON, C. R., GARDNER, J. V., MAYER, L. A., BUKTENICA, M. W., DARTNELL, P., RAMSEY, D. W. & ROBINSON, J. E. 2002. Morphology, volcanism, and mass wasting in Crater Lake, Oregon. *Geological Society of America Bulletin,* 114**,** 675-692.

BARKER, P., TELFORD, R., MERDACI, O., WILLIAMSON, D., TAIEB, M., VINCENS, A. & GIBERT, E. 2000. The sensitivity of a Tanzanian crater lake to catastrophic tephra input and four millennia of climate change. *The Holocene,* 10**,** 303-310.

BAXTER, P. J., BAUBRON, J.-C. & COUTINHO, R. 1999. Health hazards and disaster potential of ground gas emissions at Furnas volcano, Sao Miguel, Azores. *Journal of Volcanology and Geothermal Research,* 92**,** 95-106.

BEIER, C., HAASE, K. M. & HANSTEEN, T. H. 2006. Magma evolution of the Sete Cidades volcano, São Miguel, Azores. *Journal of Petrology,* 47**,** 1375-1411.

BELLEC, V., WILSON, M., BØE, R., RISE, L., THORSNES, T., BUHL-MORTENSEN, L. & BUHL-MORTENSEN, P. 2008. Bottom currents interpreted from iceberg ploughmarks revealed by multibeam data at Tromsøflaket, Barents Sea. *Marine Geology,* 249**,** 257-270.

BJÖRCK, S., RITTENOUR, T., ROSÉN, P., FRANÇA, Z., MÖLLER, P., SNOWBALL, I., WASTEGÅRD, S., BENNIKE, O. & KROMER, B. 2006. A Holocene lacustrine record in the central North Atlantic: proxies for volcanic activity, short-term NAO mode variability, and long-term precipitation changes. *Quaternary Science Reviews,* 25**,** 9-32.

BLANCO, I., GARCIA, A. & TORTA, J. M. 1997. Magnetic study of the Furnas caldera (Azores). *Annals of Geophysics,* 40.

BLOMQVIST, S. 1991. Quantitative sampling of soft-bottom sediments: problems and solutions. *Mar. Ecol. Prog. Ser.,* 72**,** 295-304.

BOOTH, B., CROASDALE, R. & WALKER, G. P. L. 1978. Quantitative Study of 5000 Years of Volcanism on Sao-Miguel, Azores. *Philosophical Transactions of the Royal Society a-Mathematical Physical and Engineering Sciences,* 288**,** 271-319.

CARMO, R., MADEIRA, J., HIPÓLITO, A. & FERREIRA, T. 2014. Paleoseismological evidence for historical surface faulting in São Miguel island (Azores). *Annals of Geophysics,* 56.

CASADEVALL, T. J., DE LA CRUZ-REYNA, S., ROSE JR, W. I., BAGLEY, S., FINNEGAN, D. L. & ZOLLER, W. H. 1984. Crater lake and post-eruption hydrothermal activity, El Chichón Volcano, Mexico. *Journal of Volcanology and Geothermal Research,* 23**,** 169-191.

CHRISTENSON, B. 2000. Geochemistry of fluids associated with the 1995–1996 eruption of Mt. Ruapehu, New Zealand: signatures and processes in the magmatic-hydrothermal system. *Journal of Volcanology and Geothermal Research,* 97**,** 1-30.

COLE, P. D., QUEIROZ, G., WALLENSTEIN, N., GASPAR, J. L., DUNCAN, A. M. & GUEST, J. E. 1995. An historic subplinian phreatomagmatic eruption: The 1630 AD eruption of Furnas volcano, Sao Miguel, Azores. *Journal of Volcanology and Geothermal Research,* 69**,** 117-135.

COLLIER, J. & BROWN, C. 2005. Correlation of sidescan backscatter with grain size distribution of surficial seabed sediments. *Marine Geology,* 214**,** 431-449.

CRUZ, J., ANTUNES, P., AMARAL, C., FRANÇA, Z. & NUNES, J. 2006. Volcanic lakes of the Azores archipelago (Portugal): Geological setting and geochemical characterization. *Journal of volcanology and geothermal research,* 156**,** 135-157.

CRUZ, J. V. L., COUTINHO, R. M., CARVALHO, M. R., OSKARSSON, N. & GISLASON, S. R. 1999. Chemistry of waters from Furnas volcano, São Miguel, Azores: fluxes of volcanic carbon dioxide and leached material. *Journal of Volcanology and Geothermal Research,* 92**,** 151-167.

DA PONTE, P. 1880. Castro EVPC (1880) -Anno de 1630. Erupção no Valle das Furnas. *Arch. Açores, 2: 527-547*.

DA PURIFICAÇÃO, M. 1880. Castro EVPC (1880) -Anno de 1630. Erupção no Valle das Furnas. *Arch. Açores, 2: 527-547*.

DIAS, U. D. M. 1936. História do Vale das Furnas. Vila-franca do Campo, Emp. Tip. Ltd. de Vila-franca do Campo.

EICHELBERGER, J. C. & GOOLEY, R. 1977. Evolution of silicic magma chambers and their relationship to basaltic volcanism. *The Earth's Crust***,** 57-77.

FARR, T. G., ROSEN, P. A., CARO, E., CRIPPEN, R., DUREN, R., HENSLEY, S., KOBRICK, M., PALLER, M., RODRIGUEZ, E. & ROTH, L. 2007. The shuttle radar topography mission. *Reviews of geophysics,* 45.

FERREIRA, T., GASPAR, J. L., VIVEIROS, F., MARCOS, M., FARIA, C. & SOUSA, F. 2005. Monitoring of fumarole discharge and CO2 soil degassing in the Azores: contribution to volcanic surveillance and public health risk assessment. *Annals of Geophysics,* 48**,** 787-796.

FONSECA, L., MAYER, L., ORANGE, D. & DRISCOLL, N. 2002. The high-frequency backscattering angular response of gassy sediments: model/data comparison from the Eel River Margin, California. *The Journal of the Acoustical Society of America,* 111**,** 2621-2631.

GARDNER, J. V., MAYER, L. A. & CLARKE, J. E. H. 2000. Morphology and processes in Lake Tahoe (California-Nevada). *Geological Society of America Bulletin,* 112**,** 736-746.

GASPAR, J. L., GOULART, C., QUEIROZ, G., SILVEIRA, D. & GOMES, A. 2004. Dynamic structure and data sets of a GIS database for geological risk analysis in the Azores volcanic islands. *Natural Hazards and Earth System Sciences,* 4**,** 233-242.

GENTE, P., DYMENT, J., MAIA, M. & GOSLIN, J. 2003. Interaction between the Mid‐Atlantic Ridge and the Azores hot spot during the last 85 Myr: Emplacement and rifting of the hot spot‐derived plateaus. *Geochemistry, Geophysics, Geosystems,* 4.

GOMES, A., GASPAR, J. L. & QUEIROZ, G. 2006. Seismic vulnerability of dwellings at Sete Cidades Volcano (S. Miguel Island, Azores). *Natural Hazards and Earth System Sciences,* 6**,** 41-48.

GONÇALVES, H. J. 1880. Castro EVPC (1880) -Anno de 1630. Erupção no Valle das Furnas. *Arch. Açores, 2: 527-547*.

GUEST, J. E., GASPAR, J. L., COLE, P. D., QUEIROZ, G., DUNCAN, A. M., WALLENSTEIN, N., FERREIRA, T. & PACHECO, J. M. 1999. Volcanic geology of Furnas Volcano, Sao Miguel, Azores. *Journal of Volcanology and Geothermal Research,* 92**,** 1-29.

HOVLAND, M. & JUDD, A. 1988. *Seabed pockmarks and seepages: impact on geology, biology, and the marine environment*, Springer.

JONES, G., CHESTER, D. & SHOOSHTARIAN, F. 1999. Statistical analysis of the frequency of eruptions at Furnas Volcano, São Miguel, Azores. *Journal of volcanology and geothermal research,* 92**,** 31-38.

LEE, S. H. & KIM, K.-H. 2004. Side-Scan Sonar Characteristics and Manganese Nodule Abundance in the Clarion—Clipperton Fracture Zones, NE Equatorial Pacific. *Marine Georesources and Geotechnology,* 22**,** 103-114.

LOURENÇO, N., MIRANDA, J., LUIS, J., RIBEIRO, A., VICTOR, L. M., MADEIRA, J. & NEEDHAM, H. 1998. Morpho-tectonic analysis of the Azores Volcanic Plateau from a new bathymetric compilation of the area. *Marine Geophysical Researches,* 20**,** 141-156.

LOWE, D. J. 2011. Tephrochronology and its application: a review. *Quaternary Geochronology,* 6**,** 107-153.
MALHEIRO, A. 2006. Geological hazards in the Azores archipelago: Volcanic terrain instability and human vulnerability. *Journal of Volcanology and Geothermal Research,* 156**,** 158-171.
MARQUES, R., QUEIROZ, G., COUTINHO, R. & ZÊZERE, J. 2007. Actividade geomorfológica desencadeada pela crise sísmica de 2005 no Vulcão do Fogo (S. Miguel, Açores): avaliação da susceptibilidade com recurso a regressão logística. *Publicações da Associação Portuguesa de Geomorfólogos,* 5**,** 47-61.
MOORE, J. G., SCHWEICKERT, R. A. & KITTS, C. A. 2014. Tsunami-generated sediment wave channels at Lake Tahoe, California-Nevada, USA. *Geosphere,* 10**,** 757-768.
MOORE, R. B. 1991a. *Geologic map of São Miguel, Azores*, US Geological Survey.
MOORE, R. B. 1991b. Geology of Three Late Quaternary Stratovolcanos of São Miguel, Azores *U.S. GEOLOGICAL SURVEY BULLETIN 1900*.
MORGAN, L., SHANKS, W., LOVALVO, D., JOHNSON, S., STEPHENSON, W., PIERCE, K., HARLAN, S., FINN, C., LEE, G. & WEBRING, M. 2003. Exploration and discovery in Yellowstone Lake: results from high-resolution sonar imaging, seismic reflection profiling, and submersible studies. *Journal of Volcanology and Geothermal Research,* 122**,** 221-242.
MOSHER, D. C. & SIMPKIN, P. G. 1999. Environmental Marine Geoscience 1. Status and Trends of Marine High-Resolution Seismic Reflection Profiling: Data Acquistion. *Geoscience Canada,* 26.
NELSON, C. H., MEYER, A. W., THOR, D. & LARSEN, M. 1986. Crater Lake, Oregon: A restricted basin with base-of-slope aprons of nonchannelized turbidites. *Geology,* 14**,** 238-241.
NEWHALL, C., PAULL, C., BRADBURY, J., HIGUERA-GUNDY, A., POPPE, L., SELF, S., BONAR SHARPLESS, N. & ZIAGOS, J. 1987. Recent geologic history of Lake Atitlan, a caldera lake in western Guatemala. *Journal of volcanology and geothermal research,* 33**,** 81-107.
OLIVER, M. A. & WEBSTER, R. 1990. Kriging: a method of interpolation for geographical information systems. *International Journal of Geographical Information System,* 4**,** 313-332.
OPPENHEIM, A. V. & COBRA, D. T. 1988. 25.4 Digital Processing of Side Scan Sonographs. *RLE Progress Report No. 130***,** 208.
POPPE, L., PAULL, C., NEWHALL, C., BRADBURY, J. & ZIAGOS, J. 1985. A geophysical and geological study of Laguna de Ayarza, a Guatemalan caldera lake. *Journal of volcanology and geothermal research,* 25**,** 125-144.
ROWE JR, G. L., OHSAWA, S., TAKANO, B., BRANTLEY, S. L., FERNANDEZ, J. F. & BARQUERO, J. 1992. Using crater lake chemistry to predict volcanic activity at Poás volcano, Costa Rica. *Bulletin of volcanology,* 54**,** 494-503.
ROWLAND-SMITH, A. 2007. The 1630 AD eruption of Furnas volcano, São Miguel, Azores (Portugal): chemical variations and magmatic processes.
SCHOCK, S. G., LEBLANC, L. R. & MAYER, L. A. 1989. Chirp subbottom profiler for quantitative sediment analysis. *Geophysics,* 54**,** 445-450.
SEARLE, R. 1980. Tectonic pattern of the Azores spreading centre and triple junction. *Earth and Planetary Science Letters,* 51**,** 415-434.
SENOS, M. L., TEVES-COSTA, P. & NUNES, J. C. 1998. SEISMICITY STUDIES OF THE AZORES ISLANDS-AN APPLICATION TO THE JULY 9, 1998 EARTHQUAKE.
SPARKS, S. R. & SIGURDSSON, H. 1977. Magma mixing: a mechanism for triggering acid explosive eruptions. *Nature,* 267**,** 315-318.
ULUSOY, İ., LABAZUY, P., AYDAR, E., ERSOY, O. & ÇUBUKÇU, E. 2008. Structure of the Nemrut caldera (Eastern Anatolia, Turkey) and associated hydrothermal fluid circulation. *Journal of Volcanology and Geothermal Research,* 174**,** 269-283.
VALADÃO, P., GASPAR, J., QUEIROZ, G. & FERREIRA, T. 1999. Landslides density map of S. Miguel Island, Azores archipelago. *Natural Hazards and Earth System Science,* 2**,** 51-56.

WALKER, G. & CROASDALE, R. 1971. Two plinian-type eruptions in the Azores. *Journal of the Geological Society,* 127**,** 17-55.

WALLENSTEIN, N., DUNCAN, A., CHESTER, D. & MARQUES, R. 2007. Fogo volcano (Sao Miguel, Azores): a hazardous edifice. *Géomorphologie: relief, processus, environnement***,** 259-270.

WARD, S. N. 2001. Landslide tsunami. *Journal of Geophysical Research: Solid Earth (1978–2012),* 106**,** 11201-11215.

WAYTHOMAS, C. F., WALDER, J. S., MCGIMSEY, R. G. & NEAL, C. A. 1996. A catastrophic flood caused by drainage of a caldera lake at Aniakchak Volcano, Alaska, and implications for volcanic hazards assessment. *Geological Society of America Bulletin,* 108**,** 861-871.

VOGT, P. & JUNG, W. 2004. The Terceira Rift as hyper-slow, hotspot-dominated oblique spreading axis: a comparison with other slow-spreading plate boundaries. *Earth and Planetary Science Letters,* 218**,** 77-90.

VÖLKER, D. J. 2010. A simple and efficient GIS tool for volume calculations of submarine landslides. *Geo-Marine Letters,* 30**,** 541-547.

YANG, T., SHEN, Y., VANDERLEE, S., SOLOMON, S. & HUNG, S. 2006. Upper mantle structure beneath the Azores hotspot from finite-frequency seismic tomography. *Earth and Planetary Science Letters,* 250**,** 11-26.

Manuscript